

Electron pair production at surfaces: Response to occupied Shockley stateF. O. Schumann,¹ C. Winkler,¹ and J. Kirschner^{1,2}¹*Max-Planck Institut für Mikrostrukturphysik, Weinberg 2, 06120 Halle, Germany*²*Institut für Physik, Martin-Luther-Universität Halle-Wittenberg, 06099 Halle, Germany*

(Received 27 June 2013; published 30 August 2013)

We have investigated the electron pair emission from a Cu(111) surface excited with a primary electron beam. We use the diffraction of electron pairs to identify the contribution of the Shockley surface state to the intensity. Exploring energy and momentum conservation laws makes it possible to select this state and to investigate the electron-electron interaction within this two-dimensional electronic system. We also find for this system the emergence of a zone of reduced intensity, which is the manifestation of the exchange-correlation hole. Furthermore, the region of reduced intensity displays an intensity pattern that reflects the symmetry of the surface.

DOI: [10.1103/PhysRevB.88.085129](https://doi.org/10.1103/PhysRevB.88.085129)

PACS number(s): 79.60.-i, 71.20.-b

I. INTRODUCTION

Upon creation of a surface, the bulk electronic properties are influenced. This can lead to the formation of new electronic states termed surface states that are spatially confined near the surface.¹⁻³ The very definition of a surface state implies that the state resides in a bulk band gap. Bulk states and a surface state can be regarded as largely decoupled electronic systems. This offers the unique opportunity to investigate a 2D electronic system. The experimental identification of these states is facilitated by photoemission experiments at different photon energies, because the energetic position of the surface state does not vary. A prominent example is the Shockley surface state of the (111) face of the noble metals Cu, Ag, and Au.³⁻⁹ This state exhibits a quadratic dispersion and two-dimensional momentum distributions prove it to be isotropic in momentum space, although the specimen is a single crystal. From this point of view, we may regard the Shockley state as an experimental realization of a two-dimensional uniform interacting electron gas.

The mutual influence of electrons is mediated by the Coulomb interaction and the Pauli principle, both can not be neglected in any electronic system. In atoms, the electron correlation is at the heart of the Hund rules, which specify the magnetic moment of atoms. In the solids, these moments can couple in a parallel/antiparallel fashion leading to the formation of ferro/antiferromagnetic order.

Exact calculations for the electronic states of atoms, molecules, and condensed matter do not exist and a key problem is to account for the electron interaction properly. A successful approximation in solid state physics is the local density approximation (LDA) within the density functional theory (DFT).¹⁰ This scheme finally leads to the formulation of the Kohn-Sham equations, which formally look like the Schrödinger equation for a single electron.¹⁰ This is the reason why an effective single-particle picture can be used. The electron-electron interaction within the LDA is approximated by the exchange-correlation energy of the interacting uniform electron gas in which the exchange-correlation (xc) hole plays a central role. An important consequence is that the xc hole is of spherical shape. Further developments of the DFT is an active field of research in which nonspherical xc holes enter.^{11,12} As an example relevant to this study we refer to a recent study of the xc hole near a Cu(100) surface.¹³

It is therefore of fundamental interest to study the properties of a uniform interacting system beyond the effective single-particle description. This is possible via electron pair emission from surfaces. The emission of electron pairs via excitation by one primary electron or absorption of one photon is only possible due to the existence of electron correlation. Hence this technique is capable to study the relative motion of electrons, which is beyond the capability of photoemission. Consequently, this lead to the development of electron coincidence spectroscopy for the investigation of atoms, molecules, and solids.¹⁴⁻²³ A key result from surface studies is the ability to observe the manifestation of the xc-hole as a depletion zone in momentum distributions. An obvious extension is to investigate the electron pair emission process from a two-dimensional electronic system like a surface state. This is aided by the surface sensitivity of the technique and the Shockley surface state is an appropriate candidate. We are motivated to focus on the Cu(111) surface state, because of the availability of pair emission calculations from this state.²⁴⁻²⁷

The theoretical treatment of pair emission via electron excitation, referred to as (e,2e) in the following, uses as input a quasiparticle band structure with the incoming primary electron being described as a LEED state.^{21,26,28} One can question the adequacy of this approach because photoemission experiments display strong deviations from a quasiparticle picture due to electron correlation effects.²⁹⁻³¹ We have demonstrated recently in an experimental (e,2e) study on a Cu(111) surface, which focused on energy distributions, that this picture is adequate for this material.³²

In this work, we utilize pair diffraction to identify the existence of the Shockley state in pair emission. In a next step, we focus on this state and investigate the momentum relations between the emitted pairs. We observe the emergence of a depletion zone in the coincidence intensity also for this 2D system. Further, the momentum presentations display the symmetry of the surface as expected from general symmetry considerations and from theoretical pair emission distributions.^{19,26,27} We also find that the emission direction of the electrons is confined to rather narrow directions in accordance with theory. In contrast to theory, we find a different azimuthal orientation of these intensity pockets.

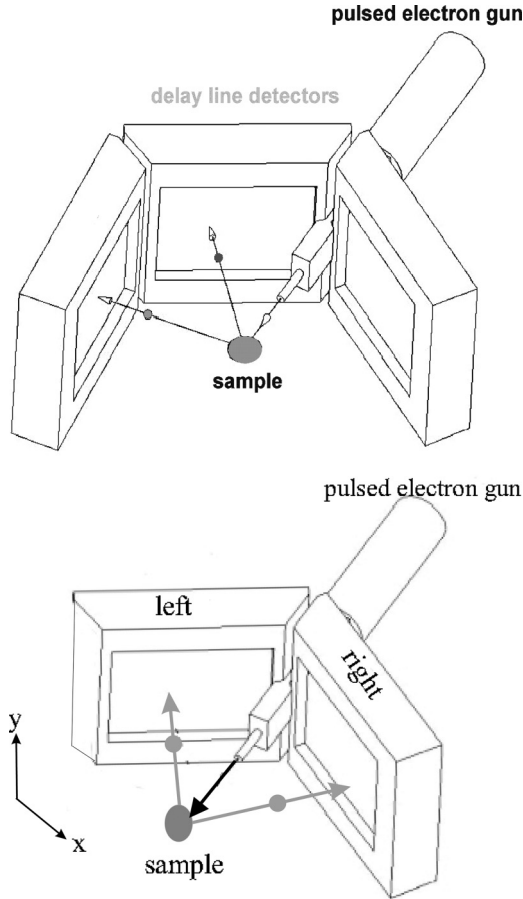


FIG. 1. Sketch of the experimental apparatus. A pulsed primary electron beam hits the sample. Emitted electrons can be detected on three channelplate detectors equipped with delay line anodes. In the case of normal incidence, only two detectors are used, because the sample blocks electron emission to the third detector. In this case, we label one detector “left” and the other “right.” The sample azimuth can be varied and data with either the $[\bar{2}11]$ or $[\bar{1}10]$ direction oriented along the x direction are presented.

II. EXPERIMENTAL DETAILS

In Fig. 1, we provide a schematic view of our experimental setup, which we described previously.³³ The experiment utilizes a time-of-flight (TOF) technique. Delay line anodes allow the determination of the impact positions of the electrons and it is possible to recover the impact positions of coincident pairs even if they hit the same detector. The angular acceptance of the instrument is $\pm 90^\circ$ in one direction while perpendicular it is $\pm 22^\circ$. If, for example, the detector on the left is omitted, the angular acceptance is reduced to $\pm 55^\circ$ versus $\pm 22^\circ$. We operate the instrument with two detectors in the case of normal incidence, because the surface blocks electron emission to the third detector. In this mode, we label the remaining detectors as “left” and “right,” respectively.

A pulsed electron beam with 2-MHz repetition rate excites the sample with a kinetic energy in the range of 28–36 eV. The electron energies are determined via the flight times and all quoted kinetic energies are referenced with respect to the vacuum level of the Cu(111) surface, which has a work function of 4.88 eV. A coincidence circuit ensures that only

one pair can be detected for each pulse. The spectrometer is part of an ultra high vacuum system equipped with standard surface science tools. Each coincident event is characterized by six parameters, namely the individual energies and the azimuthal and polar angles defining the emission direction. This allows us finally to compute the in-plane momenta of the individual electrons. The total time resolution is approximately 1.9 ns. This will lead to an energy dependent energy resolution, which is 1.0 eV for 13-eV electrons. A clean and well-ordered Cu(111) surface was prepared via Ar sputtering and annealing up to 800 K. The experiments were performed at room temperature, more details can be found elsewhere.³³

III. KINEMATICS AND IDENTIFICATION OF THE SHOCKLEY SURFACE STATE IN PAIR EMISSION

In the (e,2e) process, an electron with well-defined primary energy E_p and parallel momentum k_{\parallel}^p impinges on the surface and two electrons with kinetic energies ($E_{\text{left}}, E_{\text{right}}$) and parallel momentum ($k_{\parallel}^{\text{left}}, k_{\parallel}^{\text{right}}$) may be detected in vacuum. We have at this point the arbitrary definition to label the emitted electrons as “left” and “right.” The usefulness will become clear later. Let us discuss energy conservation first for which we find

$$E^p + E_s^N = E_s^{N-1} + E_{\text{left}} + E_{\text{right}}. \quad (1)$$

The terms E_s^N and E_s^{N-1} describe the energy of the specimen (e.g., solid sample) before and after the emission, respectively. The superscript N and $N - 1$ indicate the number of electrons within the sample. Simple rearrangement yields

$$E^p + (E_s^N - E_s^{N-1}) = E_{\text{left}} + E_{\text{right}} = E_{\text{sum}}. \quad (2)$$

For future reference, we have also defined the sum energy E_{sum} of the emitted pair. The energy terms E_s^N and E_s^{N-1} are true many-body terms because the interaction among the electrons plays a crucial role. Therefore these terms can not be a sum of single-particle energies. Nevertheless, one usually adopts an effective single electron (quasiparticle) picture and identifies the difference with a single-electron valence state E_b^v . Such a notation has proven to be a rather good starting point, however, it is a serious simplification and photoemission studies have demonstrated that many-body effects can not be excluded.^{29–31} For example, a significant broadening of the quasiparticle peaks was observed for transition metals. Another aspect is the emergence of satellites in the Ni spectra, which is not captured in the effective single-electron picture.^{34–37} Even for the supposedly simple metal Cu deviations are noted.³⁸ This raises the question whether such a quasiparticle picture can be used in pair emission spectroscopy since this technique is sensitive to the electron-electron interaction.^{21,26,28,39} Current (e,2e) theory uses such a band structure calculation as input. In the above definition of the energy term E_b^v , the work function ϕ is implicitly contained. However, it is customary to explicitly write the work function, and we finally obtain

$$E^p + E_b^v = E_{\text{sum}} + \phi. \quad (3)$$

It is obvious that for a given primary energy, only for those E_{sum} values pair intensity can be observed where the valence states has a nonvanishing density of states. Due to the fact

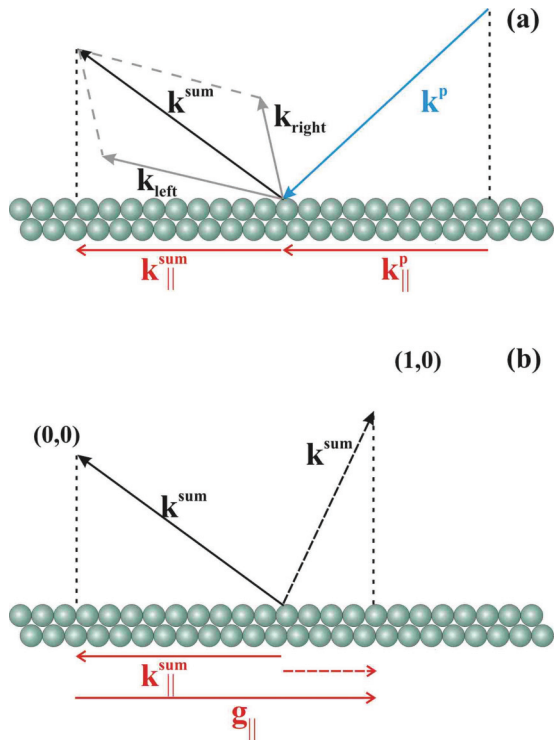


FIG. 2. (Color) Sketch of the momentum relations in pair emission. In (a), an incoming primary electron impinges onto a solid surface defined by a momentum vector \mathbf{k}^p and in-plane component $k_{||}^p$. The two outgoing electrons are characterized by momentum vectors \mathbf{k}_{left} and $\mathbf{k}_{\text{right}}$ leading to a sum momentum \mathbf{k}^{sum} and its projection into the plane $k_{||}^{\text{sum}}$. We assumed in this plot that $k_{||}^v = 0$ and a vanishing reciprocal lattice vector. According to Eq. (4), this leads to the same length of the in-plane components $k_{||}^{\text{sum}}$ and $k_{||}^p$. In (b), we display two emerging \mathbf{k}^{sum} beams, which differ in their in-plane components by a reciprocal lattice vector $\mathbf{g}_{||}$.

that the specimen is a single crystalline surface the in-plane momentum is conserved in the (e,2e) process (modulo a reciprocal lattice vector \mathbf{g}). In the same fashion as before, we introduce a quasiparticle with momentum $k_{||}^v$ and momentum conservation:

$$\mathbf{k}^p + \mathbf{k}_{||}^v = \mathbf{k}_{||}^{\text{left}} + \mathbf{k}_{||}^{\text{right}} + \mathbf{g}_{||} = \mathbf{k}_{||}^{\text{sum}} + \mathbf{g}_{||}. \quad (4)$$

From these equations, it becomes clear that by fixing the value of E_{sum} and $\mathbf{k}_{||}^{\text{sum}}$ the valence state $E_b^v(\mathbf{k}_{||}^v)$ is uniquely defined. It is this fact that enables us experimentally to identify the valence state participating in the pair emission process. In Fig. 2, we illustrate the momentum relations in a (e,2e) experiment. We have assumed in this plot $k_{||}^v = 0$ for simplicity and due to the fact that we will focus on such a state in further discussions. In Fig. 2(a), the lengths of the in-plane momentum vector of primary electron ($k_{||}^p$) and electron pair ($k_{||}^{\text{sum}}$) are the same as evidenced by the two red arrows. This in turn means that according to Eq. (4), no reciprocal lattice vector is required. In panel (b), we contrast the scenario with and without a reciprocal lattice vector. For this, we have simplified the sketch by omitting the momentum vectors of the individual electrons and of the primary beam. The components $k_{||}^{\text{sum}}$ have different lengths, but the difference is accounted for by a reciprocal lattice vector. If only one valence state (in our

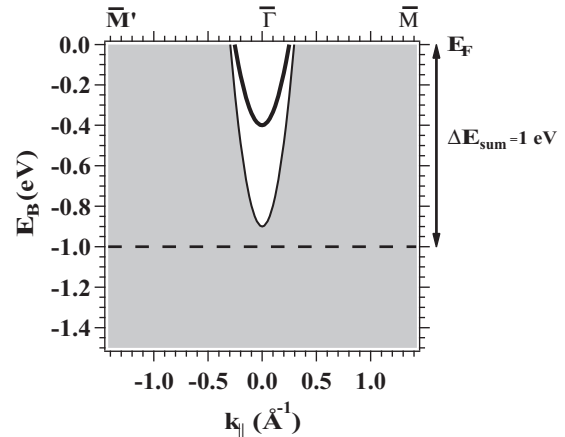


FIG. 3. Simplified band structure of Cu projected onto the (111) surface. The solid line shows the dispersion of the Shockley surface state, which exists in the bulk band gap (white area). The gray area indicates available bulk states. The dashed line marks the available valence states for $E_{\text{sum}} = 1$ eV below E_F . The arrow on the right represents the energy resolution of the experiment.

example with $k_{||}^v = 0$ and $E_b^v = 0$) is considered, the sample will emit pairs in well-defined beams. Consequently, we may label one k_{sum} beam as (0,0) and the other (0,1) in analogy to the notation in LEED. We come to the conclusion that Eq. (4) can also be interpreted as a diffraction condition for electron pairs.

If the value of $k_{||}^v$ is nonvanishing, the qualitative picture is the same in the sense that we observe the emission of well-defined k_{sum} beams, but the actual direction will shift. As long as energy conservation is fulfilled, the pair can have different values of $k_{||}^{\text{sum}}$ that differ from each other by a reciprocal lattice vector.

The minimum width of diffraction peaks using a LEED instrument is usually quoted by the so-called transfer width.⁴⁰ We can also obtain LEED images with our instrument, and we found that our instrument has a momentum resolution comparable to standard LEED optics,^{33,40} which translates into a momentum resolution of roughly 0.05 \AA^{-1} . However, another source of peak broadening is the energy resolution of the instrument. This aspect we want to discuss in the context of the Cu(111) band structure. In Fig. 3, we present a simplified sketch of the electronic states in the vicinity of E_F . The solid black curve displays the dispersion of the Shockley surface state, which has a minimum binding energy of 0.43 eV at the Brillouin zone center. This band reaches E_F for in-plane momenta $\pm 0.2 \text{ \AA}^{-1}$. The bulk band gap leading to the necks of the Cu(111) Fermi surface is marked by the white region while the gray area indicates available bulk states. Due to the fact that our energy resolution is larger than 0.5 eV, we will integrate over the full bandwidth of the surface state. Therefore our momentum resolution is limited to 0.4 \AA^{-1} . The Cu 3d states are localized in an energy window 2–5 eV below E_F , those states can be clearly excluded by an appropriate choice of E_{sum} .

Pair diffraction peaks which are characterized by a nonvanishing reciprocal lattice vector occur once the kinetic energies are sufficiently high. As to whether they can be observed depends on the angular acceptance of the instrument. If the

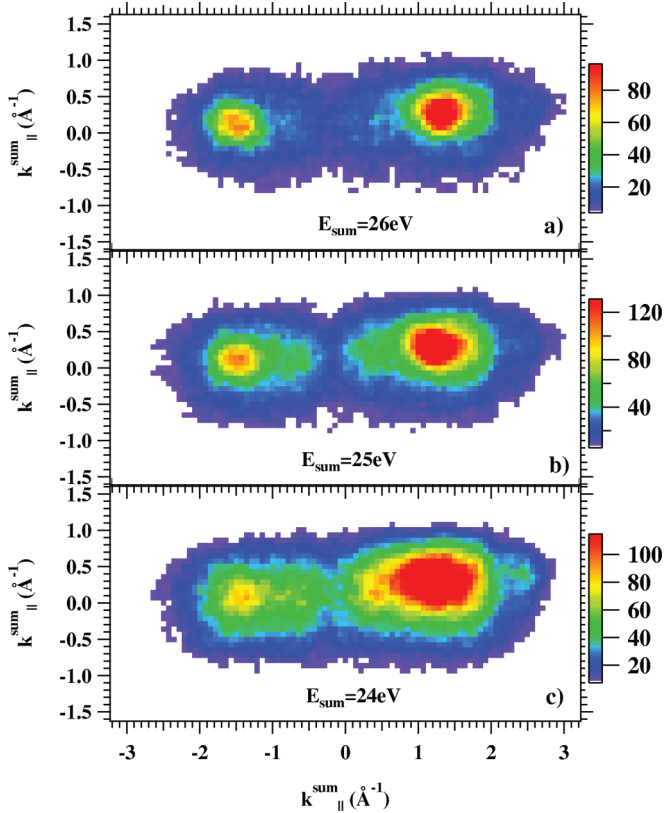


FIG. 4. (Color) 2D $k_{\parallel}^{\text{sum}}$ distribution for different values of the sum energy. The primary energy was 31 eV. The horizontal axis is along the $[\bar{2}11]$ direction, which is parallel to the shortest reciprocal lattice vector. The color code for the intensity (in counts) is displayed on the right of each plot.

peaks are outside the field of view, one needs to increase the momenta via operation at higher primary energies. However, in a TOF experiment, this leads to a degrading energy resolution, because the flight times become shorter while the time error keeps constant. The first evidence of pair diffraction was given in earlier work^{41,42} via an experiment that required operation at E_p values in the range of 80 eV. As a consequence, the energy uncertainty resulted in a momentum uncertainty of roughly 1 \AA^{-1} . In this work, we employ an instrument with an order of magnitude larger solid angle. This in turn allows the operation at lower primary energies leading to an improved energy resolution.

In Fig. 4, we display the 2D $k_{\parallel}^{\text{sum}}$ distribution obtained when the primary energy was set to 31 eV. The angle of incidence was 32° with respect to the normal. We selected the coincidence events for three different E_{sum} values within a window of ± 0.3 eV. We recall from Eq. (3) that this defines the binding energy of the valence state. Consequently, $E_{\text{sum}} = 26$ eV refers to states near E_F , whereas $E_{\text{sum}} = 25$ and 24 eV identify states 1 and 2 eV below E_F . The latter choice means that we are starting to probe the relatively flat $3d$ bands. We clearly see two prominent peaks, which become broader if E_{sum} is reduced from 26 to 24 eV but maintain their position. Obviously, the uncertainty in k_{\parallel}^v is the least for the highest possible sum energy of 26 eV. This means that there are electronic states in the vicinity of the Fermi level E_F , which are better localized in

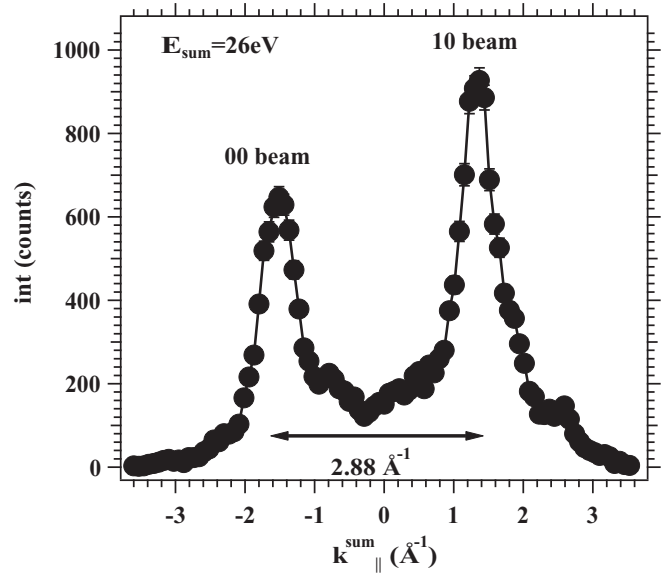


FIG. 5. Line scan along the $[\bar{2}11]$ direction through the intensity peaks of Fig. 2(a). The sum energy is 26 eV and the labeling of the spots follows the notation used in LEED, see also Fig. 2.

momentum space than those which are more than 1 eV below the Fermi level.

A line scan through the intensity peaks of Fig. 4(a) is shown in Fig. 5. The separation between the intensity maxima has a value of 2.88 \AA^{-1} , which compares favorably with the reciprocal lattice vector $g = 2.84 \text{ \AA}^{-1}$ of a Cu(111) surface. Within our coordinate system, the incoming primary electron has an in-plane momentum of -1.5 \AA^{-1} . The left peak is at this position, which means that $k_{\parallel}^v = 0$. This is qualitatively the situation depicted in Fig. 2. Hence, we identify the left intensity peak as the 00-spot in analogy to the LEED notation. Consequently, the right peak requires a reciprocal lattice vector and is labeled as the 10-spot. Both peaks have a FWHM width of about 0.5 \AA^{-1} and the intensity of the 10-spot is about 40% higher than the 00-spot. The width of the peaks is a consequence of the energy resolution as discussed above. The peak positions are determined by the kinematics described by Eq. (4), while a prediction of relative intensity levels require a dynamical calculation. We summarize that we present in Fig. 4 the diffraction of electron pairs, each characterized by the sum of their individual energies and the vector sum of their momenta.

We conclude that we have identified an initial state that has the same coordinates in energy and momentum space as the Shockley surface state. We emphasize again that this is a nontrivial observation, it supports the use of a quasiparticle band structure in $(e,2e)$ theory. Via appropriate choice of the values E_{sum} and $k_{\parallel}^{\text{sum}}$, we can focus on this state in the analysis. This ability we want to explore in the following.

IV. NORMAL INCIDENCE STUDIES

In this section, we want to discuss the results for normal incidence excitation. We aim to make contact with theoretical studies on the pair emission from a Cu(111) surface that utilizes an emission geometry as presented in Fig. 6.^{26,27} After

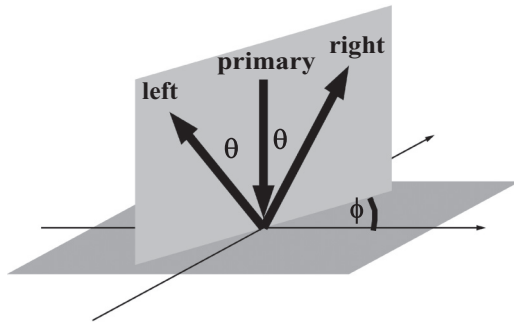


FIG. 6. Sketch of the geometry assumed by (e,2e) calculations from a Cu(111) surface.^{26,27} A normal incidence primary electron impinges onto the sample. This is followed by the emission of two electrons with equal energy and equal emission direction with respect to the surface normal. This is characterized by the angle θ while the plane containing the primary beam and the outgoing electrons has an azimuthal orientation given by ϕ .

excitation, two electrons are emitted with equal energies and with the same emission angle θ with respect to the surface normal. The primary beam and the momenta of the outgoing electrons are contained within a plane that has an azimuthal orientation ϕ with respect to a symmetry axis in the plane. The immediate consequence of this emission condition is that the valence electron has vanishing momentum k_{\parallel}^v , see Eq. (4). The experimental realization is presented in the bottom panel of Fig. 1. This means we utilize only two detectors, which we label “left” and “right,” see Fig. 1.

A. Energy and sum momentum distributions

Theory has the benefit to select a particular valence state and to determine the resulting relations among the momenta and energies of the emitted electrons. In an experiment, one can not select before the scattering event the kinetic energy and momenta of the emitted electron pair. Therefore we have to execute a series of steps to isolate these events that fulfill the emission geometry depicted in Fig. 6.

A first condition is related to the energetic position of the Shockley state, which resides in vicinity of the Fermi level. Therefore we provide a 2D energy distribution obtained with $E_p = 25.5$ eV, see Fig. 7. We have added diagonal lines to this intensity distribution. The solid line marks the position of the maximum energy $E_{\text{sum}}^{\text{max}}$ of a pair. These events are characterized by valence states with $E_b^v = 0$. From Eq. (3) and using a work function of 4.88 eV, we obtain $E_{\text{sum}}^{\text{max}} = 20.62$ eV. We can clearly observe that the coincidence intensity displays an onset. Events that lie above the solid diagonal line violate energy conservation according to Eq. (3). Therefore they have their origin in the impact of two primary electrons. This leads to the emission of two uncorrelated electrons which are termed accidental coincidences. We note in close proximity of the $E_{\text{sum}}^{\text{max}}$ diagonal an intensity band. Furthermore, we can recognize two additional intensity bands, which are marked by dashed diagonal lines. These energy positions become clearer if we compute the sum energy $E_{\text{sum}} = E_{\text{left}} + E_{\text{right}}$ of each event and show the resulting spectrum, see Fig. 8.

In order to facilitate the identification of the energy position of the valence state, we introduced an additional energy scale.

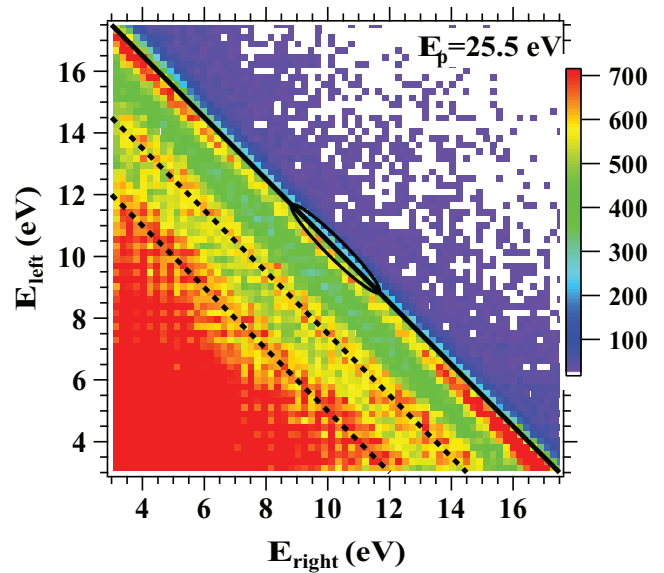


FIG. 7. (Color) 2D energy distribution obtained with $E_p = 25.5$ eV. The solid diagonal line near the onset of pair emission indicates the energetic position of $E_{\text{sum}}^{\text{max}}$. The other two dashed diagonal lines mark energy positions 3 and 5.5 eV below $E_{\text{sum}}^{\text{max}}$. Diagonal intensity bands are visible at those energy positions. The ellipse indicates the range of energies we allow for the generation of momentum plots, see Figs. 9–11. The energy position is close to $E_{\text{sum}}^{\text{max}}$ with the long axis 2.0 eV, while the short axis is 0.5 eV.

It is customary in photoemission experiments to set the energy scale such that emission from states at E_F occurs at 0 eV. If we use $E_{\text{sum}}^{\text{max}} - E_{\text{sum}}$, we obtain the same. The vertical dashed line also marks this energy position and it is apparent that the pair emission starts at $E_{\text{sum}}^{\text{max}} - E_{\text{sum}} = 0$, whereas

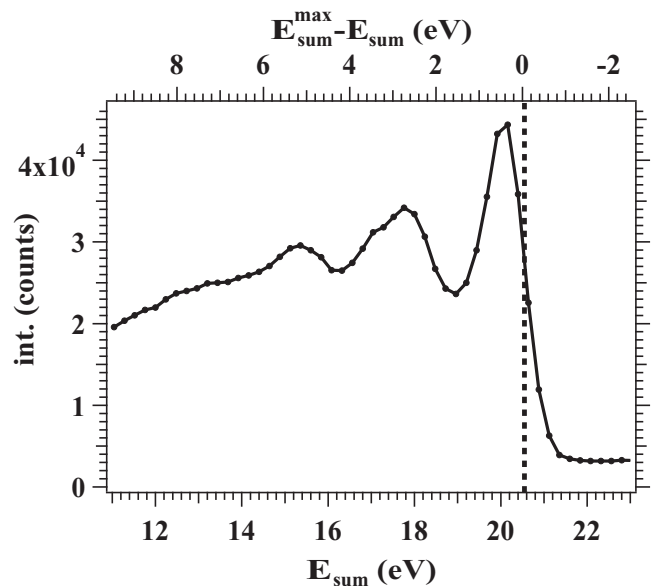


FIG. 8. Intensity vs E_{sum} spectrum obtained from the 2D energy distribution presented in Fig. 7. For an easier identification of the energetic position of the valence electron, we use $E_{\text{sum}}^{\text{max}} - E_{\text{sum}}$ as upper x axis. The position of E_F is indicated by the vertical dashed line.

a peak occurs roughly 0.5 eV below this point. Two other peaks at 3 and 5.5 eV can be identified. All three peaks are the counter part of intensity bands marked by diagonal lines in Fig. 8. These energy positions can be easily understood by the quasiparticle band structure as discussed recently.³² The emergence of diagonal lines is a consequence of the contribution of well-defined valence states in the pair emission process. This aspect was discussed in some detail in a previous study on a Cu(111) surface.³² We can confirm these findings and additionally show that the diagonal lines extend over almost the full energy window, which also agrees with the theoretical (e,2e) energy spectrum.²⁷

Obviously there is a dominant intensity near $E_{\text{sum}}^{\text{max}}$ and it is appealing to focus on these events with the additional constraint of equal individual energies. We recall that the theoretical (e,2e) work discusses emission of electrons with equal energy.^{26,27} The actual energy window we choose is determined by an ellipse, see Fig. 7. The long axis of the ellipse has a length of 2.0 eV and is aligned along the direction of fixed sum energy. The short axis is perpendicular to it and has a length of 0.5 eV. This ensures sufficient intensity for subsequent plots.

For example, we compute the two components of $k_{\parallel}^{\text{sum}}$ and show the resulting 2D distribution in Fig. 9(a). This is the equivalent of Fig. 4 for $g_{\parallel} = 0$ and we clearly observe an intensity peak centered at the origin. Due to normal incidence we conclude that this intensity refers to a valence state centered at $k_{\parallel}^v = 0$. The black lines mark the boundary of the Brillouin zone.

We label the intensity peak as 00-beam in accordance with our previous notation. Further diffraction peaks like in Fig. 4 are not observed because they are kinematically not allowed. In

order to capture them within the reduced angular acceptance of our detectors, E_p would have to exceed 60 eV. At those primary energies, the energy resolution is larger than 2 eV and the ability to separate d -band contribution from the Shockley part is lost. This finally will lead to broad spots as shown in Fig. 4. Additionally, we know from our recent work that favorable conditions to study the Shockley state are in a E_p range of 20 to 35 eV. Higher E_p values have shown to result in strongly reduced intensity near $E_{\text{sum}}^{\text{max}}$.³²

A line scan through the diffraction beam in Fig. 9(a) is shown in Fig. 9(b). This reveals that the FWHM of this peak is 0.6 \AA^{-1} . As discussed above, this width is a consequence of the energy resolution of the experiment. In lowering the E_{sum} value, the weakly dispersing d states are captured, which leads to increase of the peak width in analogy to the situation displayed in Fig. 4. The circle in Fig. 9(a) has a radius of 0.2 \AA^{-1} and marks the range we select for the momentum distributions to be shown in the next section. The radius is essentially the FWHM of the (0,0) diffraction peak and covers the part of the Brillouin zone occupied by the Shockley state.

We conclude that favorable conditions exist that allow us experimentally to approximate the scenario assumed by the theoretical (e,2e) studies on Cu(111).²⁶ Now we can investigate the momentum relation between the emitted electrons.

B. Symmetry of the electron-electron interaction

Making the energy selection as indicated by the ellipse in Fig. 7 and choosing the sum momentum of the pair via the ring in Fig. 9(a) ensures the emission geometry assumed by the theoretical studies.^{26,27} These selected coincidence events are presented in a 2D plot of the individual momenta in analogy to the calculations, see Figs. 10(b) and 10(c).

We note that for each coincident event the in-plane components of electron “left” and “right” are known. Therefore a coincidence event has an entry on the left and right halves of the plot. In this plot, we can immediately recognize the “left” and “right” detectors, respectively. The white areas are regions in momentum space that are not covered by the detectors. Outside this “blind” region, starting at about $|k_x^{l,r}| = 0.2 \text{ \AA}^{-1}$, we observe an increase of the coincidence intensity for increasing $|k_x^{l,r}|$ values. A maximum is reached at $|k_x^{l,r}| \approx 1.0 \text{ \AA}^{-1}$. The reduced intensity for small $|k_x^{l,r}|$ values is a manifestation of the xc hole as shown previously in experiment and theory.^{17,19,26,33} Here, we provide the experimental evidence that this also holds for a two-dimensional electronic system like the Shockley surface state. We may call this region of reduced intensity depletion zone. We notice that the intensity rim surrounding the depletion zone is anisotropic. There are clear intensity peaks and we have indicated in Fig. 10 that the angle between those on the left (and by symmetry also on the right) amounts to 60° . This angular periodicity is expected for a sixfold symmetric surface. An instrument with larger angular acceptance would capture six intensity peaks. If the azimuthal orientation is changed by 30° , the resulting momentum plots changes and only two of the intensity peaks are visible, see Fig. 10(c).

We conclude that the coincidence intensity reflects the sixfold symmetry of the surface. The azimuthal orientation of the sample is indicated by a sketch of the reciprocal lattice, see inset of Fig. 10. Interesting is the emergence of

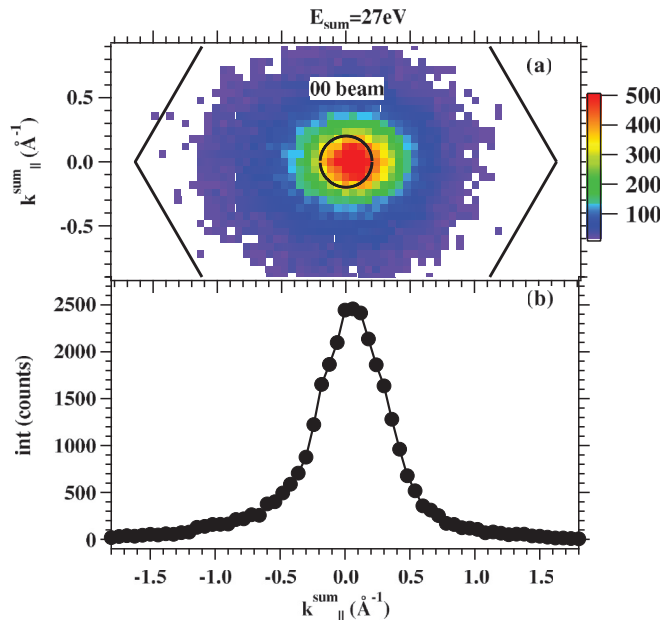


FIG. 9. (Color) In (a), we display the 2D $k_{\parallel}^{\text{sum}}$ distribution for states near $E_{\text{sum}}^{\text{max}}$. The primary energy was 32 eV. We identify the intensity peak as the 00-beam, the circle around this peak marks the momentum range we considered for the momentum plots to be shown below. The black lines indicate the Brillouin zone boundary. In (b), we show a line scan through the intensity peak.

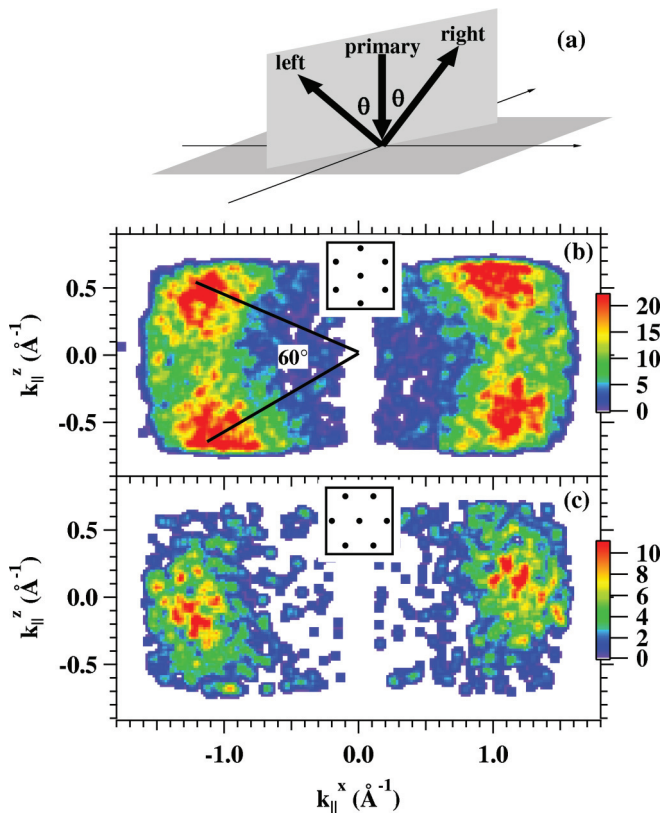


FIG. 10. (Color) (a) Emission geometry. In (b) and (c), we plot the in-plane momentum distributions for $E_{\text{left}} = E_{\text{right}} = 13$ eV at different azimuthal orientations. The horizontal axis of (b) and (c) refer to the $[\bar{1}10]$ and $[\bar{2}11]$ crystal directions, respectively. These two orientations have been indicated by insets of the reciprocal lattice within (b) and (c). The color code for the intensity (in counts) is displayed on the right.

well-defined beams, which have been predicted in a (e,2e) calculation²⁷ although the azimuthal orientation is different. In the experiment, we find that an intensity pocket is along the $[\bar{2}11]$ direction, while there is no such pocket along the $[\bar{1}10]$ direction, see Figs. 10(b) and 10(c). Theory, on the other hand, predicts the intensity peak be aligned with the $[\bar{1}10]$ direction, while no intensity peak can be found along the $[\bar{2}11]$ direction. The reason for this discrepancy is not understood.

We emphasize that these preferred emission directions are not due to diffraction of the individual electrons forming the pair. We prove this by providing a momentum distribution in which the two outgoing electrons have an energy of $E_{\text{left}} = E_{\text{right}} = 13$ eV. Different from Fig. 10 is that the coincidence condition is effectively switched off. This means that we select $E_{\text{left}} = 13$ eV and allow all values for E_{right} . This results in the left momentum distribution of Fig. 11. In the same fashion we generate the right half of Fig. 11 by selecting $E_{\text{right}} = 13$ eV while all values for E_{left} are allowed. The thus generated noncoincidence momentum distribution is rather uniform and does not reveal the emergence of a depletion zone. Furthermore, no preferred emission directions as evidenced in Figs. 10(b) and 10(c) can be observed. A preferred emission direction is only visible if we treat the pair as a single entity.

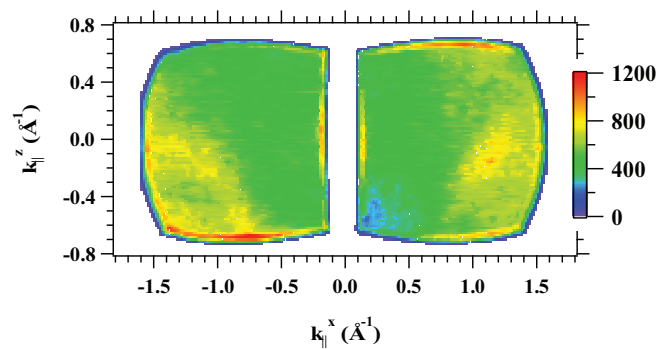


FIG. 11. (Color) Noncoincident momentum distribution. The electron energies are $E_{\text{left}} = E_{\text{right}} = 13$ eV. The color code for the intensity (in counts) is displayed on the right.

In Fig. 12, we provide an overview of momentum plots obtained with E_p values in the range 25–33 eV. The selection of the coincidence is analogous to the procedure leading to Figs. 10(b) and 11(c). This means an elliptical region centered at $E_{\text{sum}}^{\text{max}}$ and equal energies was chosen (see Fig. 7) together with the constraint that $k_{\parallel}^{\text{sum}} \leq 0.2 \text{ \AA}^{-1}$ as indicated by the circle in Fig. 9(a). For all studied energies, we observe a depletion zone. An increase of E_p leads to a higher kinetic energy of the outgoing electrons. Therefore the momentum range of the detectors increase. For the lowest primary energy of 25 eV, we observe a depletion zone, but no preferred emission direction and no clear evidence of the sixfold symmetry of the surface. Upon increasing E_p to 29 eV, we start to see the symmetry of the surface and preferred emission directions. At the highest E_p value of 33 eV, the contrast of the sixfold symmetry is strongest.

Besides, states near $E_{\text{sum}}^{\text{max}}$ emission from other energy windows are pronounced. We recall Fig. 7, which displays an additional diagonal energy band indicated by the middle diagonal dashed line. These events belong to an E_{sum} value 2.5 eV below those from the Shockley state and constitute the d band emission, see Fig. 8. We select these states by moving the ellipse shown in Fig. 7 into the region of interest. Additionally, we perform the same momentum selection $|k_{\parallel}^{\text{sum}}| \leq 0.2 \text{ \AA}^{-1}$ as previously. This finally leads to an overview of momentum distributions shown in Fig. 13. In contrast to the Shockley state, emission preferred emission directions are less apparent, only for the highest E_p value 33 eV they can be identified. The preferred emission direction is less pronounced for the d band emission, while the azimuthal alignment is the same for both valence states. Strictly speaking, we have to expect a threefold rather than a sixfold symmetry once we probe bulk bands. A similar situation arises in the LEED image from a Cu(111) surface. The first-order spots are positioned at the corners of a hexagon but display different intensity levels. Only after a 120° rotation is the same intensity recovered.

The fact that the preferred emission directions are aligned with the reciprocal lattice points, see insets in Fig. 10, suggests that diffraction plays a role. In our experiment, a primary electron propagates towards the surface, while the emitted electron pair moves away from the surface. The required momentum reversal is facilitated by the lattice. This can occur in two ways, on one hand, the primary beam is reflected in

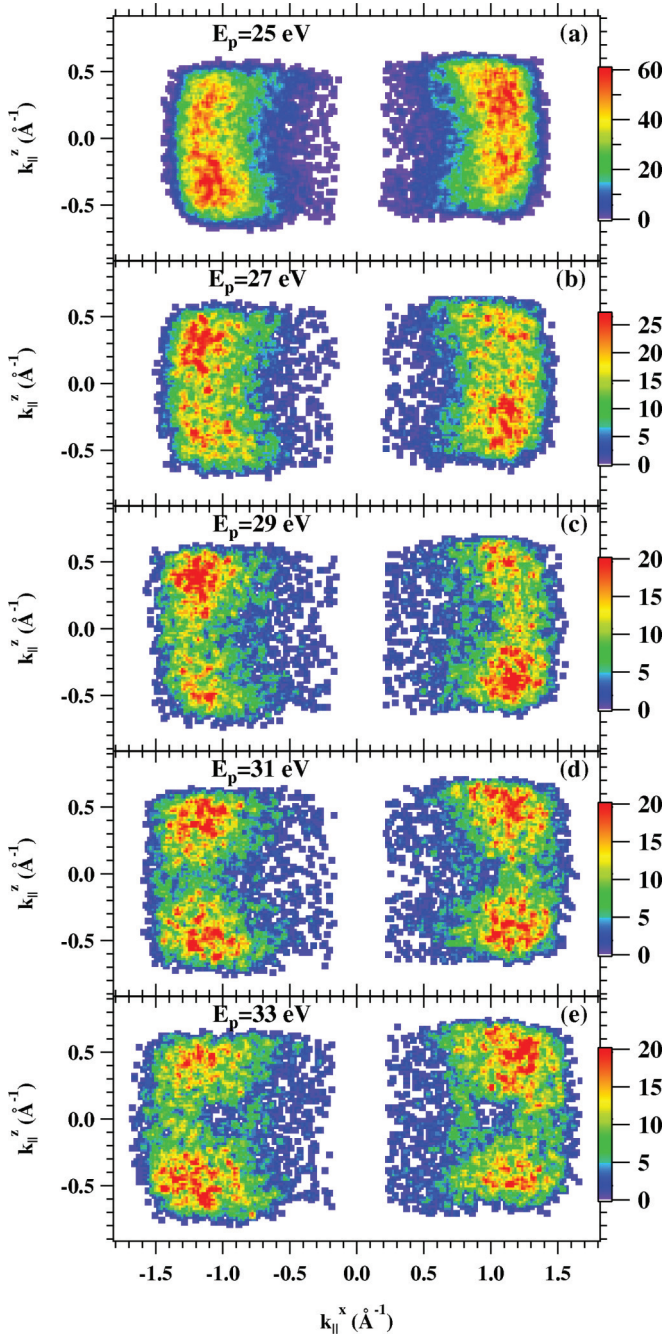


FIG. 12. (Color) An overview of momentum plots equivalent to Fig. 10 for a range of E_p values are shown. We follow an analogous procedure of energy selection and $k_{\parallel}^{\text{sum}}$ constraint. The energy constraint is depicted in Fig. 7 via the ellipse. The $k_{\parallel}^{\text{sum}}$ selection can be visualized in Fig. 9(a) via the circle. The sample azimuth is such that the $[\bar{2}11]$ direction is parallel to the x axis of the momentum. This is analogous to Fig. 10(b).

LEED beams and the actual electron-electron scattering takes place in the path towards the surface. The other possibility is that the incoming beam creates an electron pair that is scattered by the lattice. The effect of LEED is well-established, and we have demonstrated above that diffraction of pairs is a reality. These facts are cast into current (e,2e) theory.^{21,26,28} It describes the initial state via a LEED state and Bloch

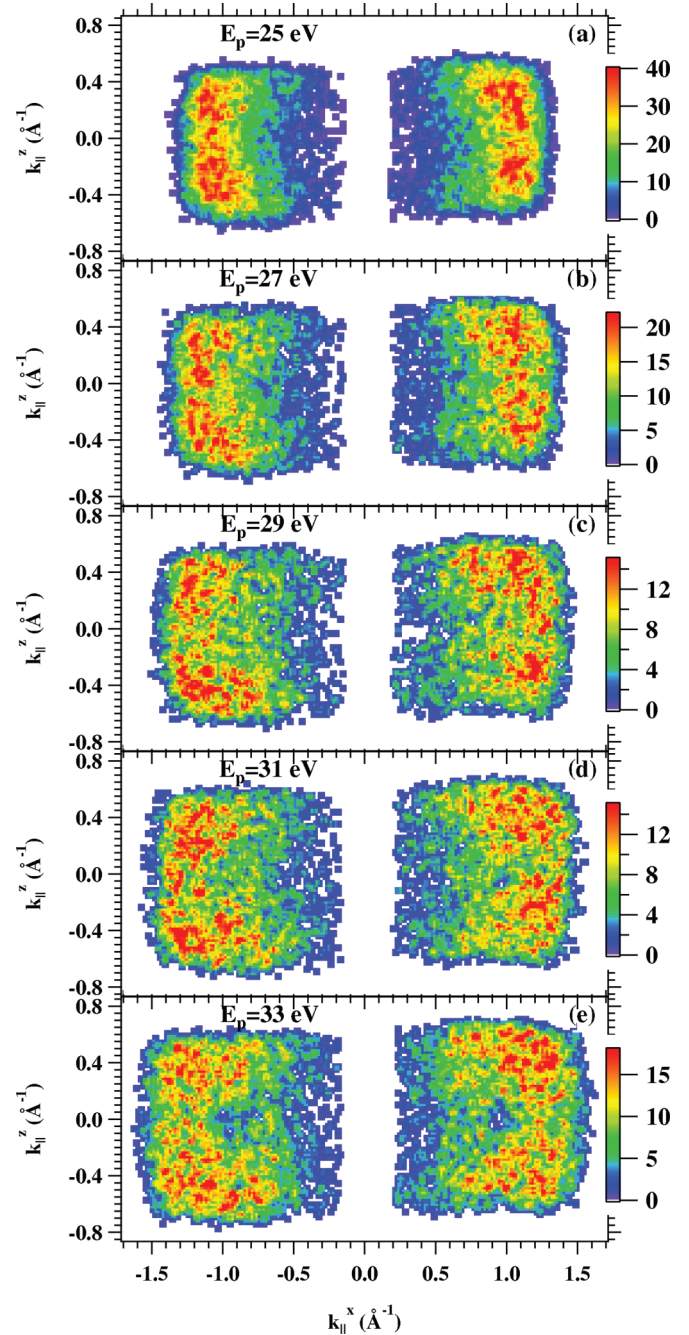


FIG. 13. (Color) These momentum plots are equivalent to Fig. 12 except that the sum energy is 2.5 eV below $E_{\text{sum}}^{\text{max}}$. This means that the ellipse defining the energy constraint is now centered at the upper dashed diagonal line in Fig. 7. With this selection we focus on the pair emission from the $3d$ states.

state for the incoming and valence electron, respectively. The two outgoing electrons are represented by time-reversed LEED states. In this multiple scattering framework, numerous pathways exist over which one has to integrate in order to get the transition probability. In Fig. 5 of Gollisch *et al.*,³⁹ a few pathways are sketched and we will focus on two aspects. Due to the fact that the primary electron is pointed towards the surface, while the outgoing electrons move away from the sample, it is obvious that a momentum reversal has taken

place. This is facilitated by the crystal lattice. For example, it is conceivable that the primary electron is elastically reflected (with or without in-plane momentum transfer) and then scatters with a valence electron. Similarly, it is possible that the incoming beam collides with a valence electron and forms a pair, with well-defined in-plane momentum and energy. Detection of this pair is only possible if this entity experiences an elastic reflection. This process exists and has been presented in this study in Fig. 4.

A E_p dependence of $(e,2e)$ spectra arises because the final state will change for a given initial state and the matrix element for the transition will be different. This may be visualized by recalling LEED I - V curves that display a strong dependence on E_p and reflexes can have low intensities. Therefore it is understandable that the preferred emission directions occur at particular E_p values, see Fig. 12. It is interesting note that first-order LEED diffraction peaks are kinematically possible for a Cu(111) surface, if the normal incident primary beam exceeds an energy of 30.8 eV. For lower primary energies, these diffraction peaks are not observed in the vacuum, but exist within the crystal. Therefore the first-order LEED beam will be almost parallel to the surface plane for E_p values near the threshold of 30.8 eV. In this case, we expect an increased Shockley state emission because this state is confined to the first 2–3 atomic layers.²⁵ However, this explanation alone brings us in conflict with momentum conservation. For normal incidence and the low values of E_p , we can ignore a reciprocal lattice vector on kinematical grounds, as discussed above. The in-plane momentum conservation of Eq. (4) can then be simplified to

$$\mathbf{k}_{\parallel}^p + \mathbf{k}_{\parallel}^v = \mathbf{k}_{\parallel}^{\text{sum}}. \quad (5)$$

If we postulate that the “effective” primary beam is a first-order LEED beam, we have included a nonzero reciprocal lattice vector on the left-hand side of Eq. (5). In order for this equation to hold, we have to add formally the same reciprocal

lattice vector on the right-hand side. This mathematical operation has an obvious physical interpretation, namely that the electron pair must experience diffraction. The existence of this is demonstrated in Fig. 4. This figure also explains why the crystal symmetry is more pronounced for the Shockley state emission (see Fig. 12) compared to the d -band emission (see Fig. 13). The pair diffraction presented in Fig. 4 is sharper for the Shockley state compared to the d -state emission. This we explained as the result of our finite energy resolution that yields sharper peaks in the case of the Shockley state compared to d -band emission. Of course, a full numerical calculation is desirable, but this is beyond the scope of this work. However, our results suggest the importance of particular pathways.

V. SUMMARY

Making use of the effect of pair diffraction we are able to identify the contribution of the Shockley surface state in the pair emission. With the appropriate choice of the energy and momentum of the pair we can focus on this 2D electronic state. We observe the formation of a zone of reduced intensity. This zone displays the symmetry of the surface. This anisotropic emission occurs into preferred directions which are aligned with the reciprocal lattice of the surface. The same alignment is also present in the case of the emission from the $3d$ band, while the contrast of the sixfold symmetry is less pronounced. Nevertheless, we prove that the depletion zone in pair emission displays the symmetry of the surface.

ACKNOWLEDGMENTS

We acknowledge the expert assistance by H. Engelhard and D. Hartung. We greatly benefited also from numerous stimulating discussions with F. Giebels, H. Gollisch, and R. Feder. Support by the DFG through SFB 272 is gratefully acknowledged.

¹I. Tamm, *Phys. Z. Sowjetunion* **1**, 733 (1932).

²W. Shockley, *Phys. Rev.* **56**, 317 (1939).

³S. Hüfner, *Photoelectron Spectroscopy* (Springer, Berlin, Heidelberg, New York, Hong Kong, London, Milan, Paris, Tokyo, 2003).

⁴P. O. Gartland and B. J. Slagsvold, *Phys. Rev. B* **12**, 4047 (1975).

⁵S. D. Kevan, *Phys. Rev. Lett.* **50**, 526 (1983).

⁶J. A. Knapp, F. J. Himpsel, and D. E. Eastman, *Phys. Rev. B* **19**, 4952 (1979).

⁷P. Heimann, J. Hermanson, H. Miosga, and H. Neddermeyer, *Surf. Sci.* **85**, 263 (1979).

⁸R. Courths and S. Hüfner, *Phys. Rep.* **112**, 53 (1984).

⁹S. G. Louie, P. Thiry, R. Pinchaux, Y. Petroff, D. Chandesris, and J. Lecante, *Phys. Rev. Lett.* **44**, 549 (1980).

¹⁰W. Kohn, *Rev. Mod. Phys.* **71**, 1253 (1999).

¹¹M. Nekovee, W. M. C. Foulkes, and R. J. Needs, *Phys. Rev. Lett.* **87**, 036401 (2001).

¹²M. Nekovee, W. M. C. Foulkes, and R. J. Needs, *Phys. Rev. B* **68**, 235108 (2003).

¹³D. B. Jochym and S. J. Clark, *Phys. Rev. B* **76**, 075411 (2007).

¹⁴L. Avaldi and A. Huetz, *J. Phys. B* **38**, S861 (2005).

¹⁵J. Ullrich, R. Moshhammer, A. Dorn, R. Dörner, L. P. H. Schmidt, and H. Schmidt-Böcking, *Rep. Prog. Phys.* **66**, 1463 (2003).

¹⁶*Correlation Spectroscopy of Surfaces, Thin Films, and Nanostructures*, edited by J. Berakdar and J. Kirschner (Wiley, Weinheim, 2004).

¹⁷F. O. Schumann, J. Kirschner, and J. Berakdar, *Phys. Rev. Lett.* **95**, 117601 (2005).

¹⁸F. O. Schumann, C. Winkler, G. Kerhervé, and J. Kirschner, *Phys. Rev. B* **73**, 041404(R) (2006).

¹⁹N. Fominykh, J. Berakdar, J. Henk, and P. Bruno, *Phys. Rev. Lett.* **89**, 086402 (2002).

²⁰F. O. Schumann, C. Winkler, and J. Kirschner, *Phys. Status Solidi B* **246**, 1483 (2009).

²¹J. Berakdar, H. Gollisch, and R. Feder, *Solid State Commun.* **112**, 587 (1999).

²²F. O. Schumann, C. Winkler, and J. Kirschner, *Phys. Rev. Lett.* **98**, 257604 (2007).

²³F. O. Schumann, C. Winkler, J. Kirschner, F. Giebels, H. Gollisch, and R. Feder, *Phys. Rev. Lett.* **104**, 087602 (2010).

- ²⁴N. Fominykh and J. Berakdar, *J. Electron. Spectrosc. Relat. Phenom.* **161**, 125 (2007).
- ²⁵N. Fominykh, J. Henk, J. Berakdar, and P. Bruno, *Surf. Sci.* **507–510**, 229 (2002).
- ²⁶H. Gollisch, N. v. Schwartzberg, and R. Feder, *Phys. Rev. B* **74**, 075407 (2006).
- ²⁷F. Giebels, H. Gollisch, and R. Feder, *J. Phys.: Condens. Matter* **21**, 355002 (2009).
- ²⁸R. Feder, H. Gollisch, D. Meinert, T. Scheunemann, O. M. Artamonov, S. N. Samarin, and J. Kirschner, *Phys. Rev. B* **58**, 16418 (1998).
- ²⁹S. Monastra, F. Manghi, C. A. Rozzi, C. Arcangeli, E. Wetli, H.-J. Neff, T. Greber, and J. Osterwalder, *Phys. Rev. Lett.* **88**, 236402 (2002).
- ³⁰J. Sánchez-Barriga *et al.*, *Phys. Rev. Lett.* **103**, 267203 (2009).
- ³¹J. Sánchez-Barriga *et al.*, *Phys. Rev. B* **82**, 104414 (2010).
- ³²F. O. Schumann, R. S. Dhaka, G. A. van Riessen, Z. Wei, and J. Kirschner, *Phys. Rev. B* **84**, 125106 (2011).
- ³³F. O. Schumann, C. Winkler, and J. Kirschner, *New J. Phys.* **9**, 372 (2007).
- ³⁴R. Clauberg, W. Gudat, E. Kisker, E. Kuhlmann, and G. M. Rothberg, *Phys. Rev. Lett.* **47**, 1314 (1981).
- ³⁵G. van der Laan, M. Surman, M. A. Hoyland, C. F. J. Flipse, B. T. Thole, Y. Seino, H. Ogasawara, and A. Kotani, *Phys. Rev. B* **46**, 9336 (1992).
- ³⁶F. Manghi, V. Bellini, J. Osterwalder, T. J. Kreutz, P. Aebi, and C. Arcangeli, *Phys. Rev. B* **59**, R10409 (1999).
- ³⁷G. van der Laan, J. Zaanen, G. A. Sawatzky, R. Karnatak, and J.-M. Esteve, *Phys. Rev. B* **33**, 4253 (1986).
- ³⁸R. Courths, M. Lau, T. Scheunemann, H. Gollisch, and R. Feder, *Phys. Rev. B* **63**, 195110 (2001).
- ³⁹H. Gollisch, X. Yi, T. Scheunemann, and R. Feder, *J. Phys.: Condens. Matter* **11**, 9555 (1999).
- ⁴⁰G. Ertl and J. Küppers, *Low Energy Electrons and Surface Chemistry* (VCH Verlag, Weinheim, 1985).
- ⁴¹J. Berakdar, S. N. Samarin, R. Herrmann, and J. Kirschner, *Phys. Rev. Lett.* **81**, 3535 (1998).
- ⁴²S. Samarin, J. Berakdar, O. M. Artamonov, H. Schwabe, and J. Kirschner, *Surf. Sci.* **470**, 141 (2000).